NANO LETTERS

pubs.acs.org/NanoLett Letter

Gold-Nanocluster-Mediated Delivery of siRNA to Intact Plant Cells for Efficient Gene Knockdown

Huan Zhang,▽ Yuhong Cao,▽ Dawei Xu, Natalie S. Goh, Gozde S. Demirer, Stefano Cestellos-Blanco, Yuan Chen, Markita P. Landry,* and Peidong Yang*

Cite This: https://doi.org/10.1021/acs.nanolett.1c01792 Read Online

ACCESS | Metrics & More | Article Recommendations | Supporting Information

ABSTRACT: RNA interference, which involves the delivery of small interfering RNA (siRNA), has been used to validate target genes, to understand and control cellular metabolic pathways, and to use as a "green" alternative to confer pest tolerance in crops. Conventional siRNA delivery methods such as viruses and *Agrobacterium*-mediated delivery exhibit plant species range limitations and uncontrolled DNA integration into the plant genome. Here, we synthesize polyethylenimine-functionalized gold nanoclusters (PEI-AuNCs) to mediate siRNA delivery into intact plants and show that these nanoclusters enable efficient gene knockdown. We further demonstrate that PEI-AuNCs protect siRNA from RNase degradation while the complex is small enough to bypass the plant cell wall. Consequently, AuNCs enable gene knockdown with efficiencies of up 76.5 ± 5.9% and 76.1 ± 9.5% for GFP and ROQ1, respectively, with no observable toxicity. Our data suggest that AuNCs can deliver siRNA into intact plant cells for broad applications in plant biotechnology.

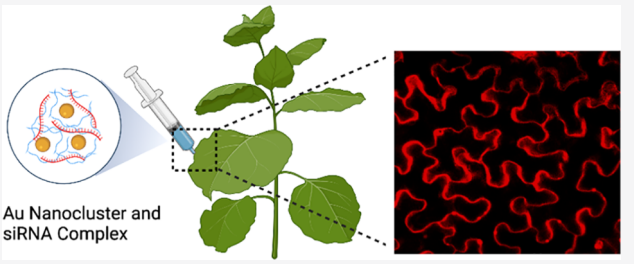

KEYWORDS: *gold nanoclusters, siRNA, delivery, gene silencing, plants*

INTRODUCTION

The emergence of RNA interference (RNAi) technologies has enabled rapid and cost-effective genetic manipulation in plant research at the level of the transcriptome for understanding cellular metabolism,[1] analyzing gene functions,[2] producing improved crop varieties,[3] and protecting crops against pests.[4] The main strategy employed in RNAi technologies is to deliver an exogenous small interfering RNA (siRNA) into the cytoplasm, which represents a significant challenge in plant-related studies.[5] In comparison with mammalian cells, mature plant cells have a thick multilayer cellulosic cell wall surrounding the cell membrane. The plant cell wall not only provides structural support and protection to plant cells but also serves as a barrier that limits biomolecule delivery and has limited the translation of other abiotic delivery methods commonly employed in mammalian systems (i.e., electroporation, heat shock, cationic lipids, positively charged polymers) to plants.[6,7] Currently, viral vectors are commonly used for the delivery of siRNA into intact plants, as they allow for strong siRNA expression without relying on plant transformation.[8] However, this method requires the construction of cDNA into the viral vectors, and most viruses are host-specific. Similarly, *Agrobacterium*-mediated transformation, the other common method for RNAi in plants, is also limited to certain plant species[9] and suffers from the additional potential drawback that random DNA integration can occur during *Agrobacterium* transformation, resulting in endogenous gene disruption and constitutive expression of the transgene.

Nanomaterial-mediated nonviral intracellular delivery has enabled numerous advances in animal research and for diverse biomedical applications.[10,11] However, due to the significant structural differences between mammalian cells and mature plant cells, these nanodelivery systems are not often directly translatable to plants. Recent work has shown that certain nanomaterials can serve as carriers to deliver plasmid DNA and RNA into intact plant cells and protoplasts.[12−19] Mitter et al. applied clay nanosheets to deliver pathogen-specific double-stranded RNA to intact leaves for crop protection against plant viruses with great success.[20] Other studies have shown that single-walled carbon nanotubes can mediate plasmid DNA delivery and transient protein expression in mature plant leaves and have also enabled highly efficient siRNA delivery and gene silencing in intact plants.[16,17] Moreover, DNA nanostructures with certain mechanical properties were able to enter cells for efficacious siRNA delivery in mature plants.[18,19] Conversely, other nanomaterials that are ubiquitously used for delivery in

Received: May 11, 2021
Revised: June 17, 2021

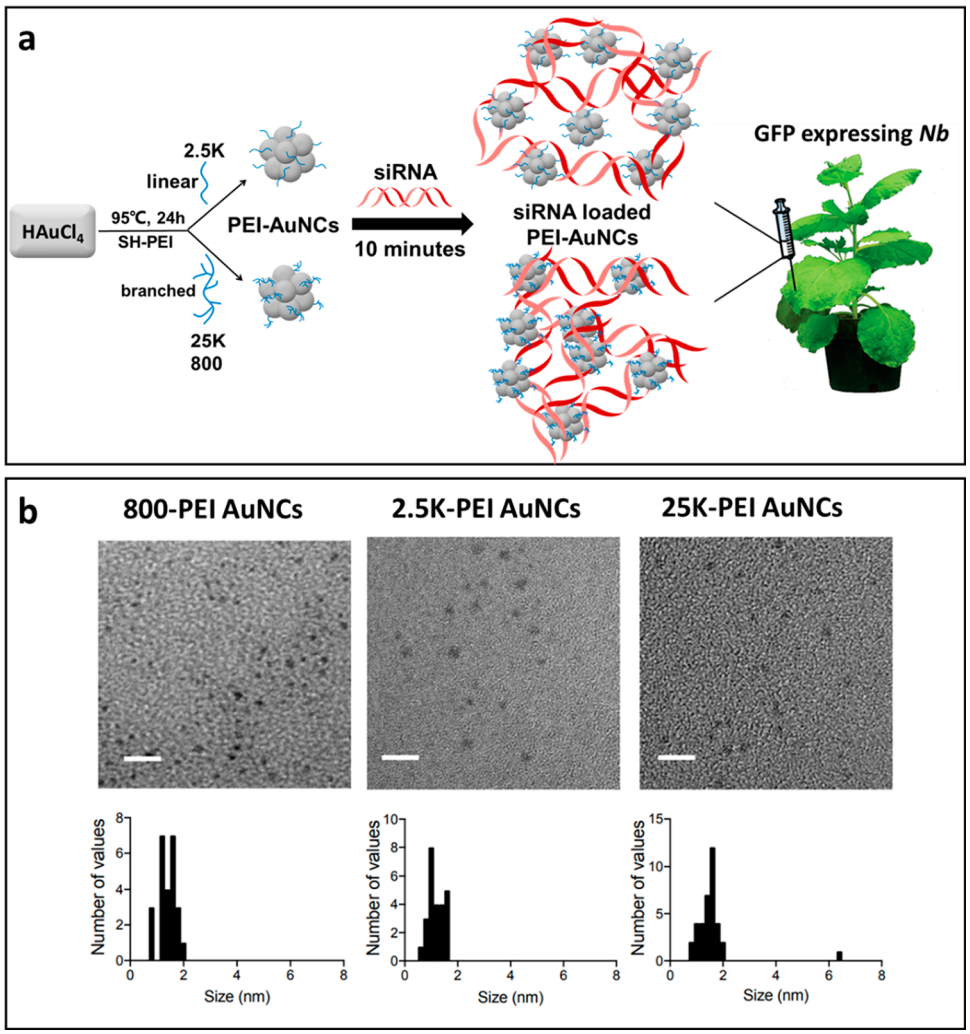

Figure 1. PEI-AuNC synthesis and characterization. (a) Schematic of PEI-AuNC synthesis (with average PEI molecular weights of 800, 2.5K, and 25K g/mol), followed by siRNA loading through electrostatic adsorption and infiltration-based delivery into mature mGFP5 *Nb* plant leaves for gene silencing. (b) TEM characterization and size distribution analysis of AuNCs modified by 800, 2.5K, and 25K PEI polymers. Scale bar: 10 nm.

animal systems such as gold nanoparticles and lipid vesicles have not yet been reported to enable biomolecule delivery in plants, which could be due in part to the plant cell wall excluding the entry of abiotic particles above the small plant cell wall size exclusion limit of ∼5−20 nm.[21,22]

Gold nanoclusters (AuNCs) have recently shown numerous successful applications in animal research. Due to their ultrasmall sizes (∼2 nm), high biocompatibility, and strong photoluminescence, AuNCs have shown great potential in intracellular delivery and diagnosis,[23−26] imaging, and energy transfer.[27,28] Previously, AuNCs were shown to be small enough to pass the bacterial cell wall and are able to interact with bacteria intracellularly to enable photosynthesis with nonphotosynthetic bacteria.[27] However, to the best of our knowledge, AuNCs have not been reported to serve as siRNA carriers in plants. In addition, AuNC synthesis is easier and faster than that of prior siRNA nanocarriers used in plant gene silencing applications. In this work, we assess whether AuNCs can serve as efficient siRNA delivery vehicles in mature plants. To this end, we synthesized polyethylenimine-functionalized AuNCs (PEI-AuNCs) with three different PEI polymer molecular weights to enable siRNA loading onto AuNCs for subsequent siRNA delivery to plant leaf tissues. We further quantified the polynucleotide loading capacity of various PEI-AuNCs, tested the DNA-loaded ability of PEI-AuNC conjugates to internalize into the cytosol of mature plant leaf cells, and quantified the resulting siRNA-mediated gene silencing efficiencies at the mRNA and protein levels. Our results below suggest that AuNCs can serve as biocompatible, easily synthesized, and efficient carriers for siRNA delivery and transient gene-silencing applications in mature plants.

RESULTS AND DISCUSSION

In this work, we first synthesized and characterized PEI-AuNCs and then validated PEI-AuNCs as an effective siRNA delivery and gene silencing platform in mature plants. siRNA was coincubated and electrostatically adsorbed onto PEI-AuNCs and then delivered via abaxial leaf infiltration to silence green fluorescent protein (GFP) transgene expression in transgenic mGFP5 *Nicotiana benthamiana* (*Nb*) plants (Figure 1a) and ROQ1 gene in wild type *Nb* plants.

Synthesis and Characterization of PEI-Functionalized Gold Nanoclusters (PEI-AuNCs). We synthesized the PEI-AuNCs with a one-step reduction of the gold precursor in the presence of three types of lipoic acid-PEI (∼2.5K g/mol linear PEI, and ∼800 g/mol and ∼25K g/mol branched PEI).[29,30]

https://doi.org/10.1021/acs.nanolett.1c01792
Nano Lett. XXXX, XXX, XXX−XXX

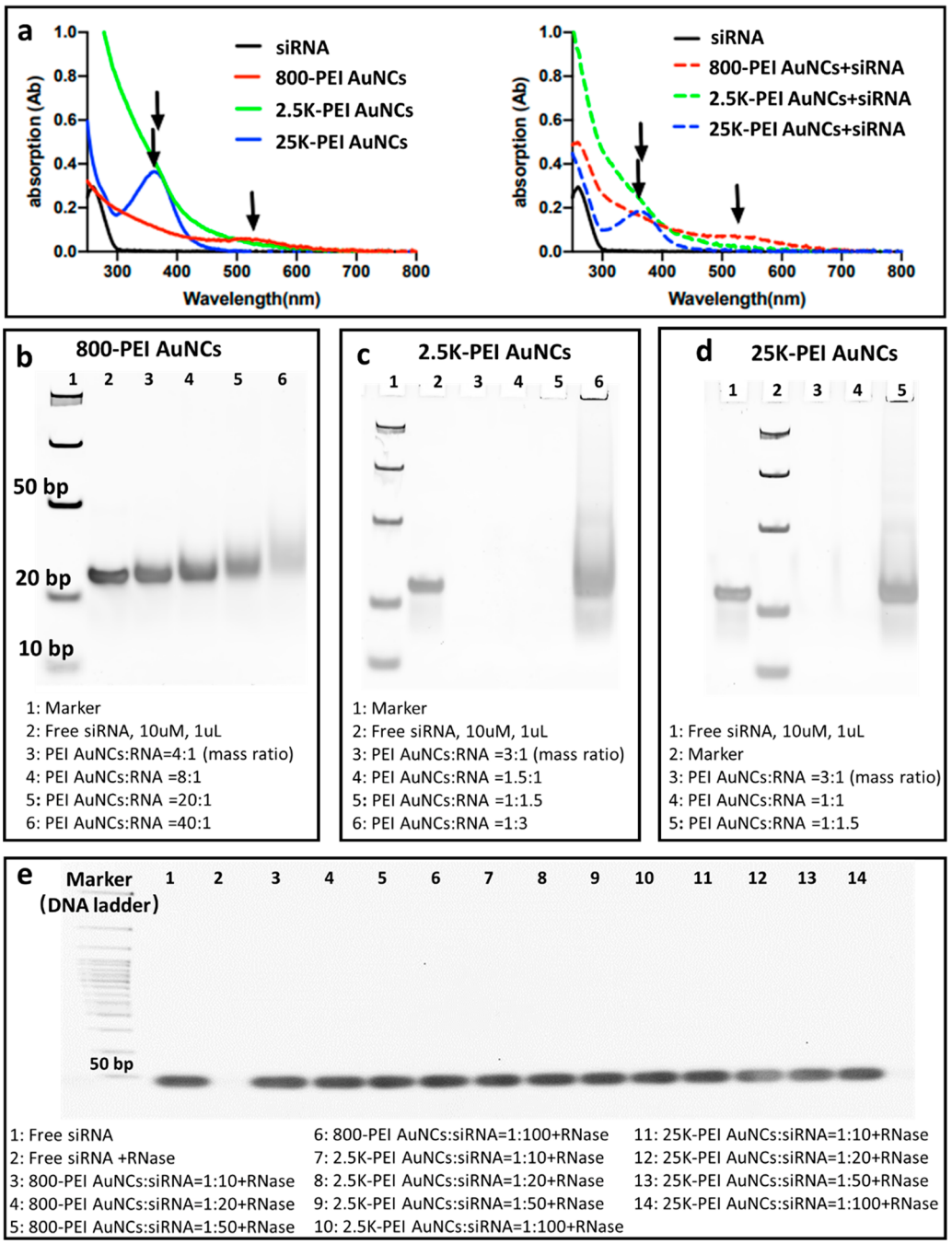

Figure 2. siRNA loading onto PEI-AuNCs and protection against nuclease degradation. (a) UV−vis absorbance spectra of PEI-AuNCs before (left) and after (right) siRNA loading (with siRNA only as a control). The corresponding characteristic peaks (black arrows) of different PEI-AuNCs do not shift following siRNA addition, indicating that the siRNA-loaded AuNCs remain homogeneous and colloidally stable after siRNA loading. (b-d) 10% native PAGE gel to quantify the siRNA loading capacity of the 800-PEI AuNCs (b), 2.5K-PEI AuNCs (c), and 25K-PEI AuNCs (d). (e) 20% native PAGE gel showing that siRNA is protected from RNase degradation after being loaded onto 800, 2.5K, and 25K PEI-AuNCs.

Lipoic acids are utilized because they can strongly coordinate onto the inorganic surfaces of gold nanocrystals and can be easily combined with tunable length polymers.[31] The 800, 2.5K, and 25K PEI-AuNCs had average positive ζ potentials of +33.63, +54.20, and +36.37 mV, respectively (Table S1), attributed to the PEI ligands that carry amine-derived positive charges. Transmission electron microscopy (TEM) images and the corresponding size distribution histograms of the PEI-AuNCs revealed that the 800, 2.5K, and 25K PEI-AuNCs were well dispersed, with sharp core structures of 1−2 nm diameter in size (Figure 1b).

PEI-AuNCs Protect Loaded siRNA against RNase Degradation. We next assessed the stability, siRNA loading efficiency, and siRNA protection capability of the three types of PEI-AuNCs. Specifically, we analyzed the UV−vis spectra of the PEI-AuNCs before and after loading siRNA to confirm the colloidal stability and incubated different amounts of siRNA with the PEI-AuNCs prior to assessing if the siRNA and PEI-AuNC complex could protect the loaded siRNA against RNase degradation.

The UV−vis spectra of the three types of PEI-AuNCs before and after loading siRNA showed the same characteristic

https://doi.org/10.1021/acs.nanolett.1c01792
Nano Lett. XXXX, XXX, XXX−XXX

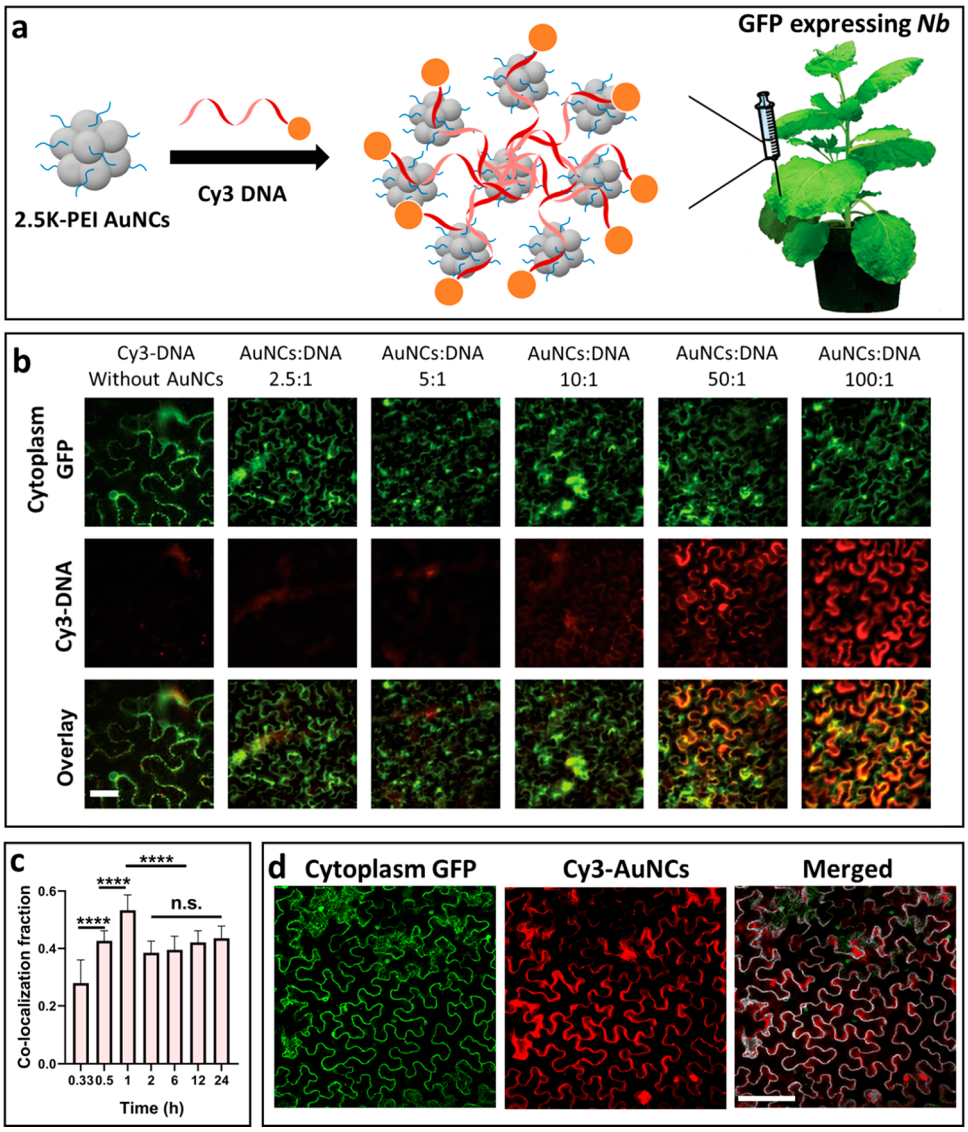

Figure 3. Internalization of Cy3-labeled 2.5K-PEI AuNCs into cells of mGFP5*Nb* leaves. (a) Representation of loading of 100 ng of Cy3-labeled single stranded DNA onto 2.5K-PEI AuNCs and infiltration into mGFP5 *Nb* plant leaves. (b) Confocal images 1 h postinfiltration showing that Cy3-DNA can enter plant cells only if it is loaded on AuNCs, with most internalization observed at AuNC:DNA mass ratios above 50:1. Scale bar: 100 μm. (c) Statistical colocalization analysis of Cy3-labeled AuNCs with cytoplasmic GFP at different incubation time points from 20 min to 24 h (****p < 0.0001 in one-way ANOVA, n.s. denotes not significant, and error bars indicate sem (n = 3)). (d) Representative confocal images (colocalized areas of the green GFP channel and red Cy3 channel are rendered in white) showing the internalization of Cy3-DNA-loaded AuNCs into mGFP5 plant cells 1 h postinfiltration. Scale bar: 100 μm.

absorption peaks at 522, 371, and 368 nm for 800, 2.5K, and 25K PEI-AuNCs,[30] respectively, indicating that PEI-AuNCs retain their chemical features and colloidal stability after siRNA loading (Figure 2a). A native PAGE electrophoresis analysis using normalized 120 ng of siRNA as a control showed that, to load 120 ng of siRNA, at least 4800 ng of 800-PEI AuNCs was required, while 80 ng of 2.5K-PEI AuNCs and 120 ng of 25K-PEI AuNCs were required, respectively (Figure 2b–d). We attribute the differences in siRNA loading capacity among the AuNCs to the inherent differences in size and charge of the constituent PEIs, which may affect the mechanism of interaction between the siRNA cargos and the PEI-AuNC carriers. Prior work showed that 100 nM siRNA is optimal for GFP transgene silencing in mGFP5 *Nb*.[17] Thus, we loaded 100 nM siRNA on PEI-AuNCs for our downstream studies. Dynamic light scattering (DLS) measurements revealed that the average hydrodynamic size of the PEI-AuNCs increased from 5–7 nm to 20–27 nm after siRNA loading (Table S1), suggesting the adsorption of siRNA to the PEI-AuNCs and the formation of a supramolecular complex. The 2.5K PEI-AuNCs loaded with siRNA were also characterized by TEM, displaying a size between 15 and 40 nm (Figure S1). Moreover, we found that siRNA loading on PEI-AuNCs contributes to an increased homogeneity of the complexes, as indicated by the lower polydispersity index (PDI) values, and does not affect the complex colloidal stability despite a lower ζ potential following siRNA addition (Table S1).

As RNA is highly susceptible to degradation, we next investigated if the three PEI-AuNCs could stabilize siRNA in the presence of RNase. We incubated either 106 ng of free siRNA or siRNA-loaded on various amounts of the three types of PEI-AuNCs with RNase H to a final concentration of 10

https://doi.org/10.1021/acs.nanolett.1c01792
Nano Lett. XXXX, XXX, XXX−XXX

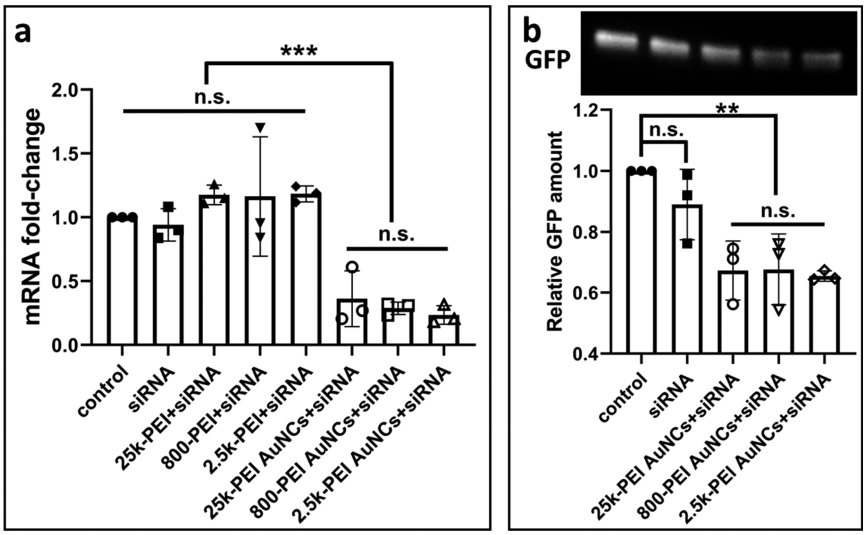

Figure 4. siRNA delivered by 800, 2.5K, and 25K PEI-AuNCs can induce efficacious gene silencing. (a) qPCR to quantify GFP mRNA fold changes 1 day postinfiltration with water (control), free siRNA, a positive control of siRNA mixed with free PEI polymers (800, 2.5K, and 25K), and siRNA-loaded PEI-AuNCs (***p = 0.004 in one-way ANOVA, n.s. denotes not significant, and error bars indicate sem (n = 3)). (b) Representative Western blot gel (top image) and statistical analysis of GFP proteins extracted from leaves treated with water (control), free siRNA, or siRNA-loaded PEI-AuNCs 3 days postinfiltration (**p = 0.0034 in one-way ANOVA. n.s. denotes not significant, and error bars indicate sem (n = 3)).

μg/mL at 37 °C for 30 min. The reaction products were then run on a 20% native page gel to quantify the relative amounts of intact versus degraded siRNA. While free siRNA was completely digested, as seen from the absence of an siRNA band in lane 2 (Figure 2e), the siRNA-loaded onto the three PEI-AuNCs was greatly protected from degradation, as shown by the persistence of an siRNA band across each lane, for a range of PEI-AuNCs:RNA loading ratios varying from 1:10 through 1:100 (lanes 3−14, Figure 2e).

Internalization of Cy3-DNA-Labeled PEI-AuNCs into Mature Plant Cells. We next tested the ability for PEI-AuNCs to internalize into the cytosol of mature mGFP *Nb* plant leaf cells. Downstream internalization experiments were performed with 2.5K-PEI AuNCs, since this nanocluster was found to have the highest loading capacity (Figure 2c). To do so, we loaded 2.5K-PEI AuNCs with a Cy3-tagged ssDNA oligo. Briefly, 100 ng of Cy3-DNA loaded onto 2.5K-PEI AuNCs was introduced into intact mGFP5 *Nb* plant leaves by infiltrating the abaxial surface of the leaf lamina with a needleless syringe (Figure 3a). Following a range of incubation times between 20 min and 24 h postinfiltration, confocal microscopy was performed on the infiltrated leaf tissues. The intrinsic GFP fluorescence of the mGFP5 *Nb* transgenic plant cells provided an intracellular fluorescent marker and thus a metric by which to assess the relative internalization efficiencies of PEI-AuNCs into plant cells: by comparing the colocalization fraction values between the cytosolic GFP channel and the Cy3 AuNC channel.

We evaluated the internalization of Cy3 PEI-AuNCs in two ways. First, we varied the mass ratio between PEI-AuNCs and Cy3-DNA from 0 to 100:1 and tested whether the PEI-AuNCs are essential for efficient cellular internalization of nucleic acids. We found that the GFP signal highly colocalizes with the Cy3 signal when the PEI-AuNC:DNA ratio is larger than 50:1, suggesting that Cy3-DNA requires the PEI-AuNC carriers for plant cell internalization (Figure 3b). Second, we tested the relative internalization efficiency of Cy3-labeled PEI-AuNCs over a series of incubation time courses from 20 min to 24 h prior to imaging the infiltrated mGFP5 *Nb* leaves. A colocalization analysis of the Cy3 fluorescence (indicating PEI-AuNCs) with the GFP fluorescence (indicating plant cell intracellular space) was used to determine the relative extent of PEI-AuNC association with plant cells and putative internalization into the plant cell cytosol. Colocalization analysis suggests that internalization becomes apparent above the baseline within 30 min (0.5 h) of infiltration with a colocalization percentage of 42.3 ± 0.5% and reaches the maximum internalization at 1 h postinfiltration with a colocalization fraction of 52.3 ± 2.1% at this time point (Figure 3c,d). As the incubation time increases beyond 1 h postinfiltration, the colocalization fraction decreases, which might be caused by the movement of PEI-AuNCs out of the cytosol or quenching of the Cy3 fluorescence in the intracellular environment. Representative confocal images in Figure S2 (for all time points) also support the colocalization trend shown in Figure 3c.

PEI-AuNCs Mediate siRNA Delivery and Induce Efficient Gene Silencing in Mature Plants. We investigated whether functional siRNA can be delivered by PEI-AuNCs to silence a constitutively expressed GFP transgene in mGFP5 *Nb* plant leaves and separately silence an endogenous ROQ1 gene in wild type *Nb* plant leaves. We selected a 21-bp siRNA sequence that targets the mGFP5 transgene as a model reporter system to evaluate the ability of PEI-AuNCs to serve as an siRNA delivery tool for transient gene silencing with 800, 2.5K, and 25K PEI-functionalized AuNCs. A 120 ng portion of this 21-bp siRNA sequence, which inhibits GFP expression in a variety of monocot and dicot plants,[32] was loaded onto the PEI-AuNCs via electrostatic adsorption at a 1:1 mass ratio for 2.5K and 25K PEI-AuNCs:siRNA and a 40:1 mass ratio for 800-PEI AuNCs on the basis of the optimal loading mass ratios of siRNA on each AuNC type. The siRNA-loaded PEI-AuNCs were then infiltrated into the abaxial side of mGFP5 *Nb* leaves prior to quantification of GFP transgene silencing.

To quantify the degree of GFP silencing, we performed a quantitative polymerase chain reaction (qPCR) of mRNA

https://doi.org/10.1021/acs.nanolett.1c01792
Nano Lett. XXXX, XXX, XXX−XXX

transcripts to evaluate the siRNA gene knockdown efficiency. mGFP5 *Nb* leaf tissues infiltrated with water, 120 ng of free siRNA, 120 ng of siRNA-loaded onto free PEI polymers, or 120 ng of siRNA-loaded PEI-AuNCs were quantified with qPCR 1 day postinfiltration. We found that that free siRNA and siRNA mixed with PEI polymers alone did not exhibit any statistically significant decreases in GFP mRNA fold changes relative to the water-infiltrated leaf control, whereas the siRNA delivered by 25K, 800, and 2.5K PEI-AuNCs showed 63.8 ± 17.8%, 71.2 ± 3.9%, and 76.5 ± 5.9% reductions in GFP mRNA transcript levels, respectively (Figure 4a). We did not observe a statistically significant difference in silencing efficiencies enabled by the different PEI-AuNCs each loaded with 120 ng of siRNA, suggesting that all three can internalize into plant cells to enable transient suppression of GFP expression. However, we noticed that the loading *efficiency* of siRNA onto PEI-AuNCs was the highest for 2.5K-PEI AuNCs and that the 2.5K-PEI AuNCs therefore may represent the best-performing AuNCs for gene silencing on an siRNA mass basis.

To further confirm that PEI-AuNCs can mediate siRNA intracellular delivery to silence GFP transgene expression, we quantified GFP levels in leaf tissues 3 days postinfiltration with siRNA-loaded PEI-AuNCs. Treated leaves were excised, proteins were extracted from ∼100 mg of treated leaf tissue, and GFP was detected and quantified with a Western blot analysis. Leaves treated with free siRNA showed the same level of GFP as the water-infiltration-treated control, whereas siRNA-loaded PEI-AuNC-treated leaves showed a statistically significant 32−35% reduction in GFP 3 days postinfiltration (Figure 4b and Figure S3).

To demonstrate that PEI-AuNCs are capable of delivering siRNA to target different genes, we targeted ROQ1,[33] an endogenous gene known to confer resistance to certain plant pathogens, using 2.5K-PEI AuNCs. We selected a 21-bp siRNA sequence that targets the ROQ1 gene and loaded this siRNA sequence onto 2.5K-PEI AuNCs via electrostatic adsorption at a 1:1 mass ratio. As with GFP silencing, qPCR results in Figure S4 show that infiltration of free siRNA into *Nb* plant leaves does not result in statistically significant decreases in ROQ1 mRNA fold changes relative to the water-infiltrated leaf controls, whereas the siRNA delivered by 2.5K-PEI AuNCs showed a 76.1 ± 9.5% reduction in ROQ1 mRNA transcript levels. Therefore, we anticipate that both endogenous genes (ROQ1) and transgenes (GFP) can be silenced with this platform and that researchers can leverage this platform to target genes of their own interest.

Finally, we tested the biocompatibility of the PEI-AuNCs with a qPCR analysis of respiratory burst oxidase homologue B (*NbrbohB*), a ubiquitous plant biotic and abiotic stress gene across many plant species.[34−37] Upregulation of *NbrbohB* can be suggestive of stress to plant tissues, and *NbrbohB* gene expression levels were thus quantified to assess the toxicity of our PEI-AuNCs. As detailed in Figure S5, a qPCR analysis of *NbrbohB* showed that both the siRNA-treated and PEI-AuNCs-treated leaves did not upregulate *NbrbohB* across three independent biological replicates, which suggests that PEI-AuNCs are biocompatible carriers for siRNA delivery to mature plants. Conversely, the siRNA-loaded PEI-AuNCs complex significantly reduced expression levels of both GFP and GFP mRNA following infiltration into mGFP5 *Nb* leaves and showed statistically insignificant changes in the levels of *NbrbohB* stress gene expression. When they are taken together, our data suggest that PEI-AuNCs serve as an efficacious platform for siRNA delivery and transient gene silencing in mature plants.

CONCLUSION

In this work, we explored the feasibility of using PEI-ligand-synthesized AuNCs as an siRNA delivery platform in mature plants. We demonstrated that the siRNA loading capacity varies greatly depending on the nature of the PEI ligand, with 2.5K linear PEI ligands enabling a loading of 1.5 μg of siRNA per 1 μg of AuNCs, relative to the lowest-performing 800 PEI ligands, which can only load 25 ng of siRNA per 1 μg of AuNCs. We further showed that PEI-AuNCs can be used as carriers for siRNA, generating efficient endogenous and transgene silencing in mature *Nb* plants (ROQ1 and GFP genes are silenced here), induced by the delivery of siRNA. Characterization of the PEI-AuNCs following infiltration into plant leaf tissues indicated that, in comparison with other nanomaterials (∼4 h for single-walled carbon nanotubes[17] and ∼12 h for DNA nanostructures[18]), PEI-AuNCs internalize into plant cells more quickly, within 0.5−1 h postinfiltration. Our data further suggest that the AuNC positive surface charge endowed by PEI ligands enables the electrostatic adsorption of polynucleotides and enables siRNA uptake into plant cells. As such, we note that the electrostatically based polynucleotide loading mechanism of siRNA onto AuNCs is likely agnostic to the polynucleotide type. Therefore, PEI-AuNCs could be a promising delivery platform for a myriad of plant biotechnology applications, potentially including AuNC-mediated delivery of other DNA or RNA cargoes, or for bioimaging and biosensing applications. In summary, our results suggest that AuNCs are a promising and biocompatible delivery platform for siRNA-mediated gene silencing in mature plants and could be implemented for diverse plant biotechnology applications.

ASSOCIATED CONTENT

Supporting Information

The Supporting Information is available free of charge at https://pubs.acs.org/doi/10.1021/acs.nanolett.1c01792.

Detailed materials and methods section (PDF)

Size and charge characterization of AuNCs, oligo sequences used in the study, representative confocal micrographs of treated plants, Western blot gels, and additional qPCR studies of AuNC endogenous gene silencing and biocompatibility (PDF)

AUTHOR INFORMATION

Corresponding Authors

Markita P. Landry − *Department of Chemical and Biomolecular Engineering, University of California, Berkeley, California 94720, United States; California Institute for Quantitative Biosciences, QB3, University of California, Berkeley, California 94720, United States; Chan Zuckerberg BioHub, San Francisco, California 94158, United States;* orcid.org/0000-0002-5832-8522; Email: landry@berkeley.edu

Peidong Yang − *Department of Materials Science and Engineering, Department of Chemistry, and Kavli Energy NanoScience Institute, University of California, Berkeley, California 94720, United States; Chemical Sciences Division, Lawrence Berkeley National Laboratory, Berkeley, California*

https://doi.org/10.1021/acs.nanolett.1c01792
Nano Lett. XXXX, XXX, XXX−XXX

94720, United States; orcid.org/0000-0003-4799-1684; Email: p_yang@berkeley.edu

Authors

Huan Zhang − *Department of Chemistry, College of Chemistry and Materials Science, Jinan University, Guangzhou, Guangdong 510632, People's Republic of China; Department of Chemical and Biomolecular Engineering, University of California, Berkeley, California 94720, United States*

Yuhong Cao − *Department of Materials Science and Engineering, University of California, Berkeley, California 94720, United States;* Present Address: CAS Key Laboratory for Biological Effects of Nanomaterials and Nanosafety, National Center of Nanoscience and Technology, 11 Zhongguancun Beiyitiao Haidian District, Beijing, China 100190.

Dawei Xu − *Department of Chemical and Biomolecular Engineering, University of California, Berkeley, California 94720, United States*

Natalie S. Goh − *Department of Chemical and Biomolecular Engineering, University of California, Berkeley, California 94720, United States*

Gozde S. Demirer − *Department of Chemical and Biomolecular Engineering, University of California, Berkeley, California 94720, United States;* Present Address: Department of Plant Biology and Genome Center, University of California, Davis, 451 Health Sciences Drive, Davis, CA 95616, USA.

Stefano Cestellos-Blanco − *Department of Materials Science and Engineering, University of California, Berkeley, California 94720, United States*

Yuan Chen − *Plant Gene Expression Center, United States Department of Agriculture-Agricultural Research Service, and Department of Plant and Microbial Biology, University of California Berkeley, Albany, California 94710, United States*

Complete contact information is available at: https://pubs.acs.org/10.1021/acs.nanolett.1c01792

Author Contributions

▽H.Z. and Y.C. contributed equally to this work.

Author Contributions

Yuhong C., H.Z., M.P.L., and P.Y. conceived the idea and designed the study. H.Z. and Yuhong C. performed the majority of the experiments and data analysis. H.Z., Yuhong C, S.C.-B., M.P.L., and P.Y. wrote or revised the manuscript. D.X. assisted in gold nanocluster synthesis. Yuan C. helped with plant seeding and maintenance. G.S.D and N.S.G. helped analyze the results. All authors edited the manuscript and approved the final version.

Notes

The authors declare no competing financial interest.

■ ACKNOWLEDGMENTS

We acknowledge support from a Burroughs Wellcome Fund Career Award at the Scientific Interface (CASI), a Stanley Fahn PDF Junior Faculty Grant under award no. PF-JFA-1760, a Beckman Foundation Young Investigator Award, a USDA AFRI award, a grant from the Gordon and Betty Moore Foundation, a USDA NIFA award, a USDA-BBT EAGER award, an NSF CAREER award, the Dreyfus Foundation, the Chan-Zuckerberg foundation, and an FFAR New Innovator Award (to M.P.L.). Work at the Molecular Foundry was supported by the Office of Science, Office of Basic Energy Sciences, of the U.S. Department of Energy under Contract No. DE-AC02-05CH11231. The authors acknowledge the support of the BASF-CARA program. We acknowledge support from the Keck Foundation (Grant 89208), and H.Z. acknowledges the support of the start-up fund from Jinan University (88016105). N.S.G. is supported by a Foundation for Food and Agriculture Research Fellowship. G.S.D. is supported by a Schlumberger Foundation Faculty for the Future Fellowship and the Resnick Sustainability Institute. The authors also acknowledge support from the UC Berkeley Molecular Imaging Center (supported by the Gordon and Betty Moore Foundation), the QB3 Shared Stem Cell Facility, and the Innovative Genomics Institute (IGI).

■ REFERENCES

(1) Agrawal, N.; Dasaradhi, P. V.; Mohmmed, A.; Malhotra, P.; Bhatnagar, R. K.; Mukherjee, S. K. RNA interference: biology, mechanism, and applications. *Microbiol. Mol. Biol. Rev.* **2003**, *67* (4), 657−85.

(2) Small, I. RNAi for revealing and engineering plant gene functions. *Curr. Opin. Biotechnol.* **2007**, *18* (2), 148−53.

(3) Tang, G.; Galili, G. Using RNAi to improve plant nutritional value: from mechanism to application. *Trends Biotechnol.* **2004**, *22* (9), 463−469.

(4) Duan, C. G.; Wang, C. H.; Guo, H. S. Application of RNA silencing to plant disease resistance. *Silence* **2012**, *3* (1), 5.

(5) Joga, M. R.; Zotti, M. J.; Smagghe, G.; Christiaens, O. RNAi Efficiency, Systemic Properties, and Novel Delivery Methods for Pest Insect Control: What We Know So Far. *Front. Physiol.* **2016**, *7*, 553.

(6) Fleischer, A.; O'Neill, M. A.; Ehwald, R. The Pore Size of Non-Graminaceous Plant Cell Walls Is Rapidly Decreased by Borate Ester Cross-Linking of the Pectic Polysaccharide Rhamnogalacturonan II. *Plant Physiol.* **1999**, *121* (3), 829−838.

(7) Schwab, F.; Zhai, G.; Kern, M.; Turner, A.; Schnoor, J. L.; Wiesner, M. R. Barriers, pathways and processes for uptake, translocation and accumulation of nanomaterials in plants–Critical review. *Nanotoxicology* **2016**, *10* (3), 257−78.

(8) Molnar, A.; Csorba, T.; Lakatos, L.; Varallyay, E.; Lacomme, C.; Burgyan, J. Plant virus-derived small interfering RNAs originate predominantly from highly structured single-stranded viral RNAs. *J. Virol.* **2005**, *79* (12), 7812−8.

(9) Crane, Y. M.; Gelvin, S. B. RNAi-mediated gene silencing reveals involvement of Arabidopsis chromatin-related genes in Agrobacterium-mediated root transformation. *Proc. Natl. Acad. Sci. U. S. A.* **2007**, *104* (38), 15156−61.

(10) Chen, F.; Zhang, G.; Yu, L.; Feng, Y.; Li, X.; Zhang, Z.; Wang, Y.; Sun, D.; Pradhan, S. High-efficiency generation of induced pluripotent mesenchymal stem cells from human dermal fibroblasts using recombinant proteins. *Stem Cell Res. Ther.* **2016**, *7* (1), 99.

(11) Stewart, M. P.; Sharei, A.; Ding, X.; Sahay, G.; Langer, R.; Jensen, K. F. In vitro and ex vivo strategies for intracellular delivery. *Nature* **2016**, *538* (7624), 183−192.

(12) Chuah, J. A.; Horii, Y.; Numata, K. Peptide-derived Method to Transport Genes and Proteins Across Cellular and Organellar Barriers in Plants. *J. Visualized Exp.* **2016**, No. 118, e54972.

(13) Sukenik, S. C.; Karuppanan, K.; Li, Q.; Lebrilla, C. B.; Nandi, S.; McDonald, K. A. Transient Recombinant Protein Production in Glycoengineered Nicotiana benthamiana Cell Suspension Culture. *Int. J. Mol. Sci.* **2018**, *19* (4), 1205.

(14) Toda, E.; Koiso, N.; Takebayashi, A.; Ichikawa, M.; Kiba, T.; Osakabe, K.; Osakabe, Y.; Sakakibara, H.; Kato, N.; Okamoto, T. An efficient DNA- and selectable-marker-free genome-editing system using zygotes in rice. *Nat. Plants* **2019**, *5* (4), 363−368.

(15) Mitter, N.; Worrall, E. A.; Robinson, K. E.; Li, P.; Jain, R. G.; Taochy, C.; Fletcher, S. J.; Carroll, B. J.; Lu, G. Q.; Xu, Z. P. Clay

nanosheets for topical delivery of RNAi for sustained protection against plant viruses. *Nat. Plants* **2017**, *3*, 16207.
(16) Demirer, G. S.; Zhang, H.; Matos, J. L.; Goh, N. S.; Cunningham, F. J.; Sung, Y.; Chang, R.; Aditham, A. J.; Chio, L.; Cho, M. J.; Staskawicz, B.; Landry, M. P. High aspect ratio nanomaterials enable delivery of functional genetic material without DNA integration in mature plants. *Nat. Nanotechnol.* **2019**, *14* (5), 456−464.
(17) Demirer, G. S.; Zhang, H.; Goh, N. S.; Pinals, R. L.; Chang, R.; Landry, M. P. Carbon nanocarriers deliver siRNA to intact plant cells for efficient gene knockdown. *Sci. Adv.* **2020**, *6* (26), No. eaaz0495.
(18) Zhang, H.; Demirer, G. S.; Zhang, H.; Ye, T.; Goh, N. S.; Aditham, A. J.; Cunningham, F. J.; Fan, C.; Landry, M. P. DNA nanostructures coordinate gene silencing in mature plants. *Proc. Natl. Acad. Sci. U. S. A.* **2019**, *116* (15), 7543−7548.
(19) Zhang, H.; Zhang, H.; Demirer, G. S.; Gonzalez-Grandio, E.; Fan, C.; Landry, M. P. Engineering DNA nanostructures for siRNA delivery in plants. *Nat. Protoc.* **2020**, *15* (9), 3064−3087.
(20) Mitter, N.; Worrall, E. A.; Robinson, K. E.; Li, P.; Jain, R. G.; Taochy, C.; Fletcher, S. J.; Carroll, B. J.; Lu, G. Q.; Xu, Z. P. Clay nanosheets for topical delivery of RNAi for sustained protection against plant viruses. *Nature Plants* **2017**, *3*, 16207.
(21) Cunningham, F. J.; Goh, N. S.; Demirer, G. S.; Matos, J. L.; Landry, M. P. Nanoparticle-Mediated Delivery towards Advancing Plant Genetic Engineering. *Trends Biotechnol.* **2018**, *36* (9), 882−897.
(22) Wang, P.; Lombi, E.; Zhao, F. J.; Kopittke, P. M. Nanotechnology: A New Opportunity in Plant Sciences. *Trends Plant Sci.* **2016**, *21* (8), 699−712.
(23) Alonso, M. C.; Trapiella-Alfonso, L.; Fernandez, J. M.; Pereiro, R.; Sanz-Medel, A. Functionalized gold nanoclusters as fluorescent labels for immunoassays: Application to human serum immunoglobulin E determination. *Biosens. Bioelectron.* **2016**, *77*, 1055−61.
(24) Yuan, Q.; Wang, Y.; Zhao, L.; Liu, R.; Gao, F.; Gao, L.; Gao, X. Peptide protected gold clusters: chemical synthesis and biomedical applications. *Nanoscale* **2016**, *8* (24), 12095−104.
(25) Lei, Y.; Tang, L.; Xie, Y.; Xianyu, Y.; Zhang, L.; Wang, P.; Hamada, Y.; Jiang, K.; Zheng, W.; Jiang, X. Gold nanoclusters-assisted delivery of NGF siRNA for effective treatment of pancreatic cancer. *Nat. Commun.* **2017**, *8*, 15130.
(26) Porret, E.; Le Guevel, X.; Coll, J. L. Gold nanoclusters for biomedical applications: toward in vivo studies. *J. Mater. Chem. B* **2020**, *8* (11), 2216−2232.
(27) Zhang, H.; Liu, H.; Tian, Z.; Lu, D.; Yu, Y.; Cestellos-Blanco, S.; Sakimoto, K. K.; Yang, P. Bacteria photosensitized by intracellular gold nanoclusters for solar fuel production. *Nat. Nanotechnol.* **2018**, *13* (10), 900−905.
(28) Zhuang, Q.; Jia, H.; Du, L.; Li, Y.; Chen, Z.; Huang, S.; Liu, Y. Targeted surface-functionalized gold nanoclusters for mitochondrial imaging. *Biosens. Bioelectron.* **2014**, *55*, 76−82.
(29) Xie, J. P.; Zheng, Y. G.; Ying, J. Y. Protein-Directed Synthesis of Highly Fluorescent Gold Nanoclusters. *J. Am. Chem. Soc.* **2009**, *131* (3), 888.
(30) Mishra, D.; Aldeek, F.; Lochner, E.; Palui, G.; Zeng, B.; Mackowski, S.; Mattoussi, H. Aqueous Growth of Gold Clusters with Tunable Fluorescence Using Photochemically Modified Lipoic Acid-Based Ligands. *Langmuir* **2016**, *32* (25), 6445−58.
(31) Chen, X. J.; Yuan, Z. F.; Yi, X. Q.; Zhuo, R. X.; Li, F. Crosslinked self-assemblies of lipoid acid-substituted low molecular weight (1800 Da) polyethylenimine as reductive-sensitive non-viral gene vectors. *Nanotechnology* **2012**, *23* (41), 415602.
(32) Tang, W.; Samuels, V.; Whitley, N.; Bloom, N.; DeLaGarza, T.; Newton, R. J. Post-transcriptional gene silencing induced by short interfering RNAs in cultured transgenic plant cells. *Genomics, Proteomics Bioinf.* **2004**, *2* (2), 97−108.
(33) Thomas, N. C.; Hendrich, C. G.; Gill, U. S.; Allen, C.; Hutton, S. F.; Schultink, A. The Immune Receptor Roq1 Confers Resistance to the Bacterial Pathogens Xanthomonas, Pseudomonas syringae, and Ralstonia in Tomato. *Front. Plant Sci.* **2020**, *11*, 463−463.
(34) Yoshioka, H.; Numata, N.; Nakajima, K.; Katou, S.; Kawakita, K.; Rowland, O.; Jones, J. D.; Doke, N. Nicotiana benthamiana gp91phox homologs NbrbohA and NbrbohB participate in H2O2 accumulation and resistance to Phytophthora infestans. *Plant Cell* **2003**, *15* (3), 706−18.
(35) Chen, X.; Yuan, Z.; Yi, X.; Zhuo, R.; Li, F. Crosslinked self-assemblies of lipoid acid-substituted low molecular weight (1800 Da) polyethylenimine as reductive-sensitive non-viral gene vectors. *Nanotechnology* **2012**, *23* (41), 415602.
(36) Nicot, N.; Hausman, J. F.; Hoffmann, L.; Evers, D. Housekeeping gene selection for real-time RT-PCR normalization in potato during biotic and abiotic stress. *J. Exp. Bot.* **2005**, *56* (421), 2907−2914.
(37) Schmittgen, T. D.; Livak, K. J. Analyzing real-time PCR data by the comparative C-T method. *Nat. Protoc.* **2008**, *3* (6), 1101−1108.

https://doi.org/10.1021/acs.nanolett.1c01792
Nano Lett. XXXX, XXX, XXX−XXX